

# Intermediate range order in vitreous silica from a partial structure factor analysis

Q. Mei and C. J. Benmore

*Argonne National Laboratory, 9700 S. Cass Avenue, Argonne, Illinois 60439, USA*

S. Sen

*Department of Chemical Engineering and Materials Science, University of California–Davis, Davis, California 95616, USA*

R. Sharma and J. L. Yarger

*Department of Chemistry and Biochemistry, Arizona State University, Tempe, Arizona 85287-1604, USA*

(Received 9 September 2008; published 20 October 2008)

By combining the methods of isotopic substitution in neutron diffraction and high-energy x-ray diffraction, we have determined partial structure factors of vitreous SiO<sub>2</sub>. A discussion of the effect of systematic and statistical errors is presented. The experimental results are found to be in good (but not exact) agreement with existing *ab initio* and classical molecular-dynamics simulations. No first sharp diffraction peak (FSDP) is observed in the concentration-concentration partial structure factor, ruling out the void-cluster-based model as a possible explanation for the origin of intermediate range order. However, the data are consistent with a model in which the intermediate range order arises from the periodicity of boundaries between a succession of small cages in the network, and the second diffraction peak is associated with chemical ordering of SiO<sub>4</sub> tetrahedra within continuous regions of the network between cages. The cage model is used to explain compositional trends in the FSDP height for neutron and x-ray data on BeO-SiO<sub>2</sub> glasses.

DOI: [10.1103/PhysRevB.78.144204](https://doi.org/10.1103/PhysRevB.78.144204)

PACS number(s): 61.43.Fs, 61.05.fm, 61.05.cp

## I. INTRODUCTION

Intermediate range order arising from preferred orientational correlations beyond the nearest-neighbor distances in chemically ordered network glasses has been discussed in the literature for many years; see reviews by Wright<sup>1</sup> and Elliott.<sup>2</sup> Elliott defined “medium range order” as covering the region of  $\sim 5\text{--}10$  Å, although longer “extended chemical ordering” up to 40 Å has also been found in network glasses.<sup>3</sup> Wright<sup>1</sup> rationalized the ordering in single-component network glasses on both of these length scales as being consistent with the “*random network theory of Zachariasen*”<sup>4</sup> for glasses provided the word “random” is replaced with “disordered.” In the Wright model, the extent of intermediate (or medium) range ordering arises from planes of successive cage walls defined by “the limit of distortion of the local structural unit and the allowed distribution of bond and bond torsion angles.”<sup>5</sup> Alternatively, Elliott<sup>2</sup> associated intermediate range order with the “chemical ordering of interstitial voids around cation-centered clusters.” In this paper we focus on testing these models of the origin of intermediate range order in SiO<sub>2</sub> glass, by performing the necessary neutron and x-ray experiments required for a full partial structure factor analysis.

Diffraction studies on vitreous silica have long been used to test structural models since the pioneering work of Warren *et al.*<sup>6</sup> in the 1930s. However a full partial structure factor analysis of vitreous SiO<sub>2</sub> has remained elusive because a “low contrast in the neutron-scattering lengths of isotopes precludes a complete determination of its structure.”<sup>7</sup> In this regard, it is particularly important to note that in covalently bonded networks such as SiO<sub>2</sub>, the first sharp diffraction peak (FSDP) at position  $Q_1$  in neutron- and x-ray-diffraction

patterns has often been associated with the existence of intermediate range order, with a periodicity of  $2\pi/Q_1$ . For binary AX<sub>2</sub>-type glasses the FSDP can be identified as having a value of  $Q_1 r_1 \sim 2.5$ ,<sup>8,9</sup> where  $r_1$  is the position for the nearest-neighbor bond length. The extraction of the partial structure factors enables the identification of the element-specific topological and chemical ordering contributions to the total diffraction patterns.<sup>3,7,10</sup> These partials provide a rigorous test of different structural models, particularly with regard to the nature of the intermediate range structural origin of the FSDP in glasses, which has been a long-standing and controversial debate in the literature.<sup>1–10</sup>

In this paper, we report the successful measurement of the partial structure factors of vitreous SiO<sub>2</sub> obtained using the method of isotopic substitution in neutron diffraction combined with high-energy x-ray diffraction. Our results suggest that for vitreous SiO<sub>2</sub> the FSDP is not caused by chemical short range ordering of interstices around cation-centered clusters. However, significant contributions to the FSDP from the oxygen-related partials suggest that intermediate range order in glassy SiO<sub>2</sub> can be related to the periodicity of the boundaries between small adjacent structural cages of SiO<sub>4</sub> tetrahedra, and the second (principal) peak to chemical ordering of SiO<sub>4</sub> tetrahedra in the regions between cages. This latter model also explains the compositional variation in the FSDP intensity observed in neutron and x-ray measurements on “stuffed” BeO-SiO<sub>2</sub> glasses, where Be and O atoms are able to fill voids in the silicate network without altering it, suggesting that the intermediate range order in silicate glasses is strongly influenced by the size and shape of cages within the network.

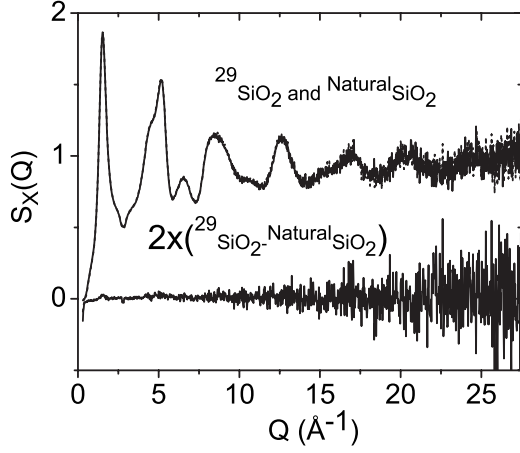


FIG. 1. The measured total x-ray structure factors  $S_X(Q)$  for the  $^{\text{Nat}}\text{SiO}_2$  (dashed line, top) and  $^{29}\text{SiO}_2$  (solid line, top) samples and the difference between them (bottom curve).

## II. EXPERIMENTAL

Glasses of 99.9% isotopically enriched  $^{29}\text{SiO}_2$  (Isoflex) and natural  $^{\text{Nat}}\text{SiO}_2$  (fumed silica, Aldrich) were prepared in an identical manner by heating the powder in a molybdenum crucible to  $2050 \pm 100$  °C in a radio-frequency furnace, under a helium atmosphere, and subsequently quenching the melt by shutting off the furnace power. Glasses produced with a quench rate of  $\sim 50$  K/s had masses of 0.7 g ( $^{29}\text{SiO}_2$ ) and 1.0 g ( $^{\text{Nat}}\text{SiO}_2$ ). High-energy x-ray-diffraction measurements were performed on 11 ID-C at the Advanced Photon Source, Argonne National Laboratory using an incident beam energy of 115 KeV and an energy-discriminating solid-state Ge detector. The x-ray data were analyzed using atomic form factors  $f(Q)$ , using the software-analysis package ISOMER-X (Ref. 11) to obtain the normalized intensity  $I_X(Q)$ . We note that previous studies on vitreous  $\text{GeO}_2$  have concluded that the shifts from the centers of the electron distributions from the nuclei are not serious in the case of oxide glasses,<sup>12,13</sup> although there is undoubtedly a small effect. The x-ray structure factors for the  $^{29}\text{SiO}_2$  and  $^{\text{Nat}}\text{SiO}_2$  samples shown in Fig. 1.

Neutron-diffraction measurements on the same isotopic samples were performed on the Glass, Liquid and Amorphous Materials Diffractometer at the Intense Pulsed Neutron Source, Argonne National Laboratory, which has a low background and high detector stability. Sample runs between  $^{\text{Nat}}\text{SiO}_2$  and  $^{29}\text{SiO}_2$  glasses contained in vanadium cans were interleaved to reduce systematic errors in the neutron differ-

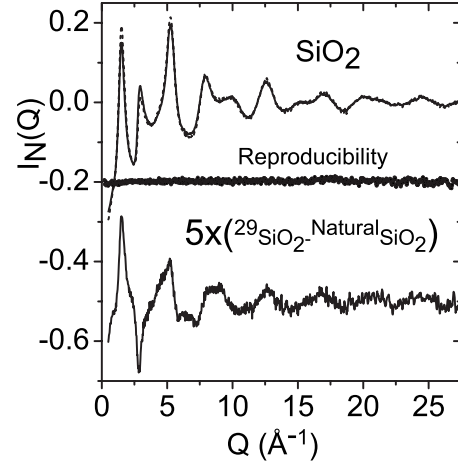


FIG. 2. The measured neutron structure factors  $I_N(Q)$  for the  $^{\text{Nat}}\text{SiO}_2$  (solid line, top) and  $^{29}\text{SiO}_2$  (dashed line, top) samples and the first-order difference (solid bottom line) shifted by 0.5. The middle line (circles) labeled “reproducibility” represents the measured difference on the same sample between the first and last runs shifted by 0.2.

ence measurement. The neutron data were analyzed using the ISAW software-analysis package<sup>14</sup> to obtain the normalized neutron intensities  $^{\text{Nat}}I_N(Q)$  and  $^{29}I_N(Q)$ . Figure 2 shows the measured neutron-diffraction data for the same glassy  $^{\text{Nat}}\text{SiO}_2$  and  $^{29}\text{SiO}_2$  samples run in the x-ray experiment.

The neutron data were analyzed using scattering lengths of  $b(\text{O})=5.803(4)$  fm and  $b(^{\text{Nat}}\text{Si})=4.1491(10)$  fm.<sup>15</sup> By extracting the first-order difference function between the  $^{\text{Nat}}\text{SiO}_2$  and  $^{29}\text{SiO}_2$  total structure factors,<sup>10</sup>

$$\Delta I(Q) = ^{29}I_N(Q) - ^{\text{Nat}}I_N(Q) \quad (1)$$

(shown in Fig. 2), and by imposing the constraint that all silicon atoms are tetrahedrally coordinated by oxygen at a distance of 1.61 Å, it was found that the scattering length for  $^{29}\text{Si}$  was  $b(^{29}\text{Si})=4.80(5)$  fm, as illustrated in Fig. 3. This is just at the error limit of the previously reported value of  $b(^{29}\text{Si})=4.70(10)$  fm.<sup>16</sup>

## III. PARTIAL STRUCTURE FACTOR ANALYSIS

To extract all the three partial structure factors for vitreous  $\text{SiO}_2$ , it is necessary to perform three independent diffraction measurements. In our case there are two neutron  $^{\text{Nat}}I_N(Q)$  and  $^{29}I_N(Q)$  spectra and one x-ray  $I_X(Q)$  spectrum. The matrix for extracting the Faber-Ziman partial structure factors,<sup>17</sup> as outlined in Ref. 18, is given below:

$$\begin{bmatrix} ^{\text{Nat}}I_N(Q) \\ ^{29}I_N(Q) \\ I_X(Q) \end{bmatrix} = \begin{bmatrix} c_{\text{Si}}^2 {}^{\text{Nat}}b_{\text{Si}}^2 & 2c_{\text{Si}}c_{\text{O}} {}^{\text{Nat}}b_{\text{Si}}b_{\text{O}} & c_{\text{O}}^2 b_{\text{O}}^2 \\ c_{\text{Si}}^2 {}^{29}b_{\text{Si}}^2 & 2c_{\text{Si}}c_{\text{O}} {}^{29}b_{\text{Si}}b_{\text{O}} & c_{\text{O}}^2 b_{\text{O}}^2 \\ c_{\text{Si}}^2 f_{\text{Si}}^2(Q) & 2c_{\text{Si}}c_{\text{O}} f_{\text{Si}}(Q)f_{\text{O}}(Q) & c_{\text{O}}^2 f_{\text{O}}^2(Q) \end{bmatrix} \cdot \begin{bmatrix} S_{\text{SiSi}}(Q) - 1 \\ S_{\text{SiO}}(Q) - 1 \\ S_{\text{OO}}(Q) - 1 \end{bmatrix}, \quad (2)$$

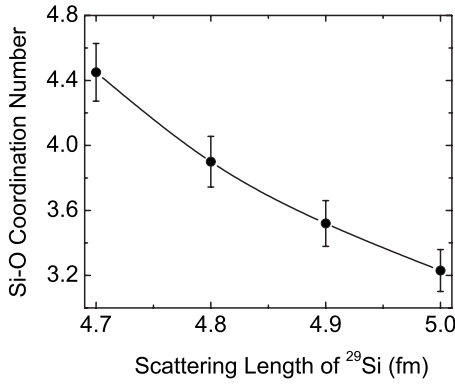


FIG. 3. The Si-O coordination number obtained from the first-order neutron difference function versus the scattering length of  $^{29}\text{Si}$ . We note that previously measured x-ray and neutron coordination numbers in tetrahedral  $\text{SiO}_2$  glass are systematically slightly less than 4 (3.8–3.9 for neutrons in Table II of Ref. 9) due to difficulties in integrating the tail of the sinc function which overlaps with the O-O peak. Allowing for this we suggest that the  $^{29}\text{Si}$  coherent-scattering length is closer to 4.8 fm.

where

$$I_X(Q) = \langle F \rangle^2 \cdot S_X(Q) = S_X(Q) \sum_{i,j=\text{Si,O}} c_i c_j f_i(Q) f_j(Q) \quad (3)$$

and

$$I_N(Q) = 4\pi\bar{b}^2 S_N(Q). \quad (4)$$

In such an analysis it is important to take into account the influence of systematic as well as statistical errors since these will amplify at the partial structure factor level. In Fig. 1 the x-ray spectra for the normal and  $^{29}\text{Si}$  isotopically enriched glasses were found to be essentially identical, the maximum difference being 0.5% at  $Q=1.5 \text{ \AA}^{-1}$ . Figure 2 gives an indication of the high level of reproducibility between neutron runs on the same sample. Figure 4 shows the Faber-Ziman partial structure factors extracted using an average of the  $^{\text{Nat}}\text{SiO}_2$  and  $^{29}\text{SiO}_2$  samples (to

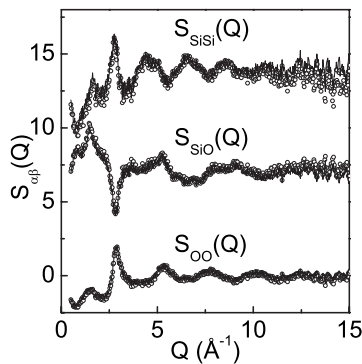


FIG. 4. The Faber-Ziman partial structure factors extracted using an average of the x-ray measurements on the  $^{\text{Nat}}\text{SiO}_2$  and  $^{29}\text{SiO}_2$  samples (line), displaced for clarity. This is compared to the same partials extracted using the same matrix method using only the  $^{\text{Nat}}\text{SiO}_2$  x-ray data (circles) to demonstrate the (low) level of systematic error in the experiment.

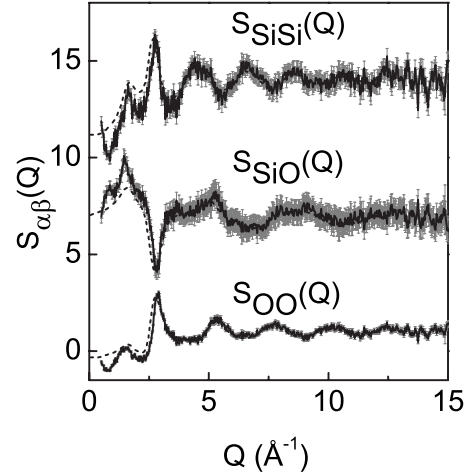


FIG. 5. Measured partial structure factors by Faber and Ziman (Ref. 17) for  $\text{SiO}_2$  glass with error bars [ $S_{\text{SiSi}}(Q)$  is displaced by +13 and  $S_{\text{SiO}}(Q)$  by +6 for clarity ( $\alpha, \beta = \text{Si, O}$ )], compared to the molecular-dynamics simulation results of Ref. 20 (dashed line). Error bars are shown in gray.

improve statistics), compared to the same partials extracted using the same method using only the  $^{\text{Nat}}\text{SiO}_2$  x-ray data. All these tests give an indication of the (relatively low) level of systematic errors introduced by using two different samples, validating the assumption that the  $^{\text{Nat}}\text{SiO}_2$  and  $^{29}\text{SiO}_2$  samples have essentially the same structure. The same partials are shown again in Fig. 5 with statistical error bars. These results confirm that all three partials contribute to the FSDP. The tabulated values for the curves in Fig. 1 have been provided as auxiliary material.<sup>19</sup>

## IV. RESULTS AND DISCUSSION

### A. Average bond angles in $\text{SiO}_2$ glass

Figure 5 compares the measured Faber-Ziman partial structure factors with those predicted by the molecular-dynamics (MD) simulation of Vashishta *et al.*<sup>20</sup> There is generally excellent agreement for  $Q > 3 \text{ \AA}^{-1}$ , with some small but noticeable shifts in peak positions and shapes for  $Q < 3 \text{ \AA}^{-1}$ . The differential distribution functions  $D_{\alpha\beta}(r) = 4\pi r [G_{\alpha\beta}(r) - 1]$ , where  $G(r)$  is the pair distribution function, correspond to the Fourier transforms of the partial structure factors  $S_{\alpha\beta}(Q)$  shown in Fig. 6. Table I compares the peak positions and coordination numbers from partial radial distribution functions to both *ab initio* MD and classical MD simulations.<sup>20–22</sup> The coordination numbers are in excellent agreement with classical MD simulations, although the peak positions show some small discrepancies. The peak positions from the measured partial pair distribution functions are consistent with the published neutron data<sup>23</sup> but slightly lower than published x-ray data (see Table II of Ref. 1). Wright<sup>1</sup> previously pointed out that a small discrepancy between neutron and x-ray results exists outside of the experimental uncertainties, and attributed this to variations in the atomic Si and O electron distributions using the x-ray data reduction procedure to describe the covalently bonded

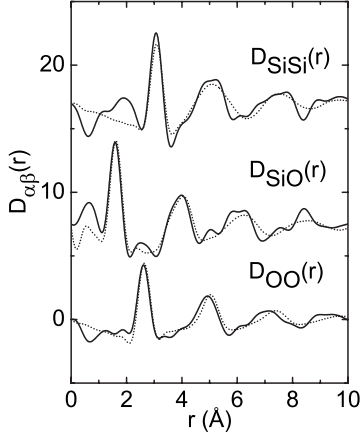


FIG. 6. The partial differential distribution functions  $D_{\alpha\beta}(r) = 4\pi\rho r[G_{\alpha\beta}(r) - 1]$  by Faber and Ziman (Ref. 17) for vitreous  $\text{SiO}_2$  (solid line), compared to the results from classical molecular dynamics (Ref. 20) (dotted line), where  $\alpha, \beta = \text{Si}, \text{O}$ .  $D_{\text{SiSi}}(r)$  is displaced by +17 and  $D_{\text{SiO}}(r)$  by +7 for clarity. Both data were truncated at  $Q_{\text{max}} = 12 \text{ \AA}^{-1}$  and Fourier transformed using a Lorch modification function (Ref. 1).

network. Figure 6 shows a comparison of the experimental partial radial distribution functions with those obtained using classical MD simulations.<sup>20</sup> All three partial structure factors show small systematic shifts at low  $Q$ . In real space the most significant difference is an  $\sim 3\%$  increase in the position of the intertetrahedral O-O peaks beyond 4  $\text{\AA}$  in the simulation data.

The torsion angles  $\alpha_1$  ( $\angle \text{Si-Si-O}$ ) and  $\alpha_2$  ( $\angle \text{Si-O-O}$ ) (shown in Fig. 16 of Ref. 1) define the local connectivity between  $\text{SiO}_4$  tetrahedra. The average angles were determined to be  $\alpha_1 = 114.7 \pm 1.5^\circ$  and  $\alpha_2 = 143.5 \pm 2.0^\circ$  based on the peak positions in the partial radial distribution functions, assuming that the Si-O bond-length and bond-angle distributions are uncorrelated.<sup>24,25</sup> We can infer information on the intermediate range order by estimating the average ring size distribution based on the extracted average  $\angle \text{Si-O-Si} = 148.5 \pm 2.0^\circ$ . This angle, the partial distribution functions, and hence the Si-O-Si bond-angle distribution are all in reasonable agreement with the reverse Monte Carlo model formulated by Kohara and Suyuza<sup>13</sup> based on simultaneous fitting of neutron and x-ray total structure factors, where the average  $\angle \text{Si-O-Si}$  is found to be  $146^\circ$  with a full width half maximum of  $17^\circ$ . As reported by previous authors,<sup>1</sup> of all the crystalline  $\text{SiO}_2$  polymorphs  $\beta$ -cristobalite is most consistent with our results for vitreous silica, where  $\angle \text{Si-O-Si} = 146.7^\circ$

and  $\angle \text{Si-Si-Si} = 109.5^\circ$  are associated with only six-membered rings. However a distribution of ring sizes may be expected in the glass and Rino *et al.*<sup>26</sup> compared the average interatomic distances and bond angles for different  $n$ -fold rings ( $n=3-10$ ) in vitreous  $\text{SiO}_2$  using configurations from molecular-dynamics simulations. The most common ring sizes found in their simulation were  $n=5, 6$ , and  $7$ , yielding an average  $\angle \text{Si-O-Si}$  angle of  $142.6^\circ$ , which is significantly lower than our results. *Ab initio* molecular-dynamics simulations by Sarnthein *et al.*<sup>21,22</sup> indicated an even lower value of  $\angle \text{Si-O-Si} = 136^\circ$ . Better agreement is found with a first-principles  $^{29}\text{Si}$  NMR analysis which found an  $\angle \text{Si-O-Si}$  of  $151^\circ$  (Ref. 27) and two-dimensional  $^{17}\text{O}$  dynamic-angle spinning NMR which gives  $\angle \text{Si-O-Si}$  of  $147^\circ$ .<sup>28</sup>

## B. Models of the origin of the FSDP in $\text{SiO}_2$ glass

The origin of the FSDP in vitreous  $\text{SiO}_2$  has long been debated in the literature.<sup>1-10</sup> Quasicrystalline models have been rejected by several authors as a viable explanation of the FSDP since no single crystalline polymorph can adequately reproduce all the features of the diffraction pattern.<sup>1,2</sup> Similarly layered structures often found in crystalline analogs of chalcogenide glasses have been found to provide an inappropriate description of the FSDP in vitreous  $\text{SiO}_2$ .<sup>1,2,8</sup> Probably the two most widely used explanations for the FSDP in vitreous  $\text{SiO}_2$  were those proposed by Wright<sup>1</sup> and Moss and Price<sup>8</sup> and by Elliott.<sup>2,12</sup>

Wright<sup>1</sup> associated the first sharp diffraction peak in vitreous silica with “the periodicity arising from the boundaries between a succession of the cages which comprise the structure of a three-dimensional covalent network.” A schematic diagram of this interpretation based on the random network glass model of Zachariasen<sup>4</sup> is shown in Fig. 7. In this scenario the cages are described as “irregular groups of 10–20 atoms enclosing the empty regions of the network,”<sup>29</sup> and three element-specific partial structure factors may be expected to contribute in the region of the FSDP, particularly the oxygen-related partials due to the high concentration of oxygen.

Elliott<sup>2,12</sup> on the other hand proposed that “the FSDP in the structure factor of network glasses and liquids is a pre-peak in the concentration-concentration structure factor [ $S_{\text{CC}}(Q)$  using the Bhatia-Thornton formalism<sup>30</sup>] due to the chemical ordering of interstitial voids around cation-centered clusters.” The notion of chemical ordering of anions and cations is illustrated in Fig. 7 by means of different colored atoms. Similarly, void-void interactions are represented, al-

TABLE I. The experimental (Expt.) peak positions and coordination numbers (obtained by integrating to the first minima of the radial distribution function), compared to those from existing MD simulations.

	Si-Si		Si-O		O-O	
	Expt.	MD	Expt.	MD	Expt.	MD
Peak position ( $\text{\AA}$ )	$3.08 \pm 0.01$	$3.10, ^a 2.98^b$	$1.60 \pm 0.01$	$1.62^{a,b}$	$2.62 \pm 0.01$	$2.64, ^a 2.68^b$
Coordination number	$4.06 \pm 0.20$	$4^a$	$3.89 \pm 0.20$	$4^a$	$5.99 \pm 0.30$	$6^a$

<sup>a</sup>Reference 20.

<sup>b</sup>Reference 21.

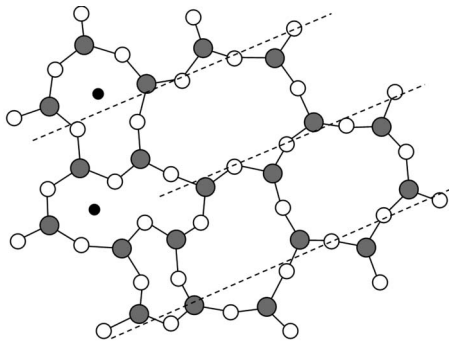


FIG. 7. A schematic of the random network model of Zachariasen (Ref. 4) for an oxide glass modified from Refs. 5 and 36. In this simplified two-dimensional (2D) illustration, the oxygen atoms are white and the Si atoms are gray. The small black circles represent possible sites for the Be atoms incorporated into the network. The planes show successive cage walls associated with intermediate range order in the model of Price *et al.* (Ref. 36). The chemical ordering arises from correlations between atoms of the same “color.”

though void-cation cluster interactions do not correlate with the Zachariasen model network.<sup>5</sup> The void-cluster model is based on two main observations, first the representation of Bletry<sup>31</sup> that “shows the structure of tetravalent monoatomic amorphous materials can be represented approximately as a mixture of spherical atoms and holes, having the same diameter and concentration, arranged in a packing which maximizes the local chemical short range order of holes and atoms,”<sup>12</sup> and second that a FSDP in  $S_{CC}(k)$  will arise from pronounced void-cation cluster ordering in real space.

Price *et al.*<sup>9</sup> argued that the FSDP originates from the competition between the rapidly decreasing form factor for the structural unit (a  $\text{SiO}_4$  tetrahedron in this case) and a rising structure factor associated with the packing of these units. In the cage model of Wright<sup>1</sup> for  $\text{SiO}_2$  therefore,  $S_{CC}(Q)$  is not required to exhibit a prepeak but significant contributions to the FSDP would originate from the  $S_{\text{SiO}}(Q)$  and  $S_{\text{OO}}(Q)$  partials, in addition to cation-cation correlations. The cage-model interpretation is therefore supported by our results shown in Fig. 1. In the void-cluster model the FSDP is ascribed to a prepeak in the concentration-concentration partial structure factor  $S_{CC}(Q)$ .<sup>2,12</sup> The first partial structure factor determination of vitreous  $\text{GeO}_2$  originally showed a slightly negative dip in the region of the FSDP.<sup>7</sup> However, recently more accurate measurements on vitreous  $\text{GeO}_2$  showed a small prepeak in  $S_{CC}(Q)$ .<sup>10</sup> *Ab initio* molecular dynamics on the other hand show no FSDP in  $S_{CC}(Q)$  for vitreous  $\text{SiO}_2$ .<sup>21</sup> Later simulations on liquid  $\text{SiO}_2$  do show a FSDP in  $S_{CC}(Q)$ , but the authors suggested that this was not necessarily associated with void-cluster correlations.<sup>32</sup> In this study we find no indication of an FSDP in the measured  $S_{CC}(Q)$  shown in Fig. 8, providing evidence against the void-cluster model as an explanation for the origin of the FSDP and associated intermediate range order in vitreous  $\text{SiO}_2$ . In Fig. 8 we also compare our measured Bhatia-Thornton partial structure factors with those calculated using *ab initio* molecular dynamics,<sup>21,22</sup> which show very good agreement given the detailed level of comparison.

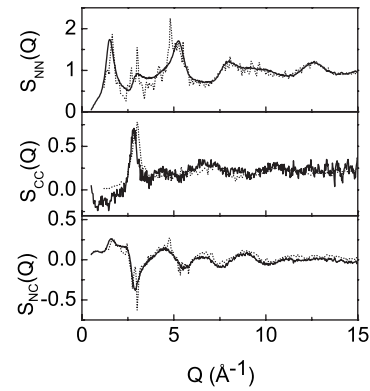


FIG. 8. A comparison of measured partial structure factors by Bhatia and Thornton (Ref. 30) (solid line) with those predicted by *ab initio* molecular-dynamics simulations (Ref. 22) (dotted line).

The (second) principal peak lies at  $Q_2=2.80 \text{ \AA}^{-1}$  for  $\text{SiO}_2$ , and it can be seen from Fig. 8 that this peak is dominated by  $S_{CC}(Q)$ , indicating chemical ordering on a length scale of  $2\pi/Q_2=2.24 \text{ \AA}$ . We note that in real space, a negative peak in  $g_{CC}(r)$  expresses a preference for unlike nearest neighbors, while a positive peak expresses a preference for like nearest neighbors.<sup>33</sup> Within the cage model of  $\text{SiO}_2$ , this second peak represents the periodicity associated with regions of continuous packing of tetrahedra between cages, which is intimately linked to chemical ordering and the local Si-O-Si and O-Si-O bond-angle distributions.

### C. Be silicate glasses

While we stress that this is by no means a general result, since the origin of the FSDP can vary from system to system, we note that the void-cluster model has been very successful in explaining the remarkable difference in the neutron FSDP height for alkali silicate glasses. Here, the scaling factor for  $S_{CC}(Q)$  (and  $S_{NC}$ ) has been varied by filling voids in the silicate network with different modifier atoms using molecular-dynamics simulations.<sup>34</sup> Lee and Elliott<sup>34</sup> found that modifier atoms with a positive neutron-scattering length, such as  $\text{Na}^+$ , result in a smaller void-cluster contrast and the FSDP intensity correspondingly decreases, whereas those with negative scattering lengths, such as  $\text{Li}^+$ , create a greater contrast and result in an increase in intensity of the FSDP. However, in practice the drawback of incorporating these ions is that they are known to depolymerize the  $\text{SiO}_2$  network. Hence, structural changes associated with the changing network are also expected.

We have investigated this effect experimentally by performing neutron and x-ray diffraction on BeO- $\text{SiO}_2$  glasses. The addition of up to 20% BeO into  $\text{SiO}_2$  has been shown by NMR to enter the silicate framework with no significant increase in nonbridging oxygens, keeping the  $\text{SiO}_2$  network intact (although strained), with  $\text{BeO}_4$  tetrahedra forming clusters within the voids.<sup>35</sup> The neutron-diffraction data on BeO- $\text{SiO}_2$  glasses, which are very sensitive to the positive neutron-scattering lengths of the added Be and O atoms, show an approximately linear decrease in the neutron FSDP intensity with decreasing  $\text{SiO}_2$  content at low BeO concen-

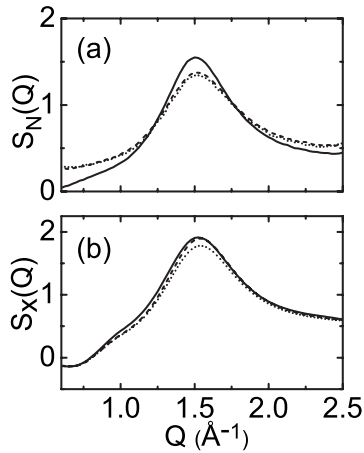


FIG. 9. The measured FSDPs in the (a) neutron and (b) x-ray total structure factors for pure  $\text{SiO}_2$  glass (solid line), 10%BeO-90% $\text{SiO}_2$  glass (dashed line), and 20%BeO-80% $\text{SiO}_2$  glass (dotted line).

trations, i.e., a 15% reduction for 15% BeO as shown in Figs. 9(a) and 10. The x-ray-diffraction data, which are far less sensitive to the contributions of the electrons on the additional Be and O atoms than the corresponding neutron data, show only a 7% reduction in the x-ray FSDP intensity with up to 20% BeO added to the voids of an unmodified network [Figs. 9(a) and 10]. These results alone are consistent with the predictions of both the void-cluster model and the cage model. However given the elimination of the void-cluster model as a viable explanation for intermediate range order in glassy  $\text{SiO}_2$ , it is argued that the reduction in FSDP intensity in BeO- $\text{SiO}_2$  (and possibly other silicate glasses) is most likely due to changes in the distribution of cage sizes and shapes within the three-dimensional (3D) network.

The diffraction data support the  $\text{SiO}_2$  network stuffed with  $\text{BeO}_4$  tetrahedra interpretation based on NMR data, by the indication of the formation of Be-rich nanoclusters in the form of three-membered rings. The x-ray data in Fig. 11 show hardly any changes in the radial distribution function except around 1.6 and 2.64  $\text{\AA}$  which varies slightly with composition, strongly suggesting that the higher- $r$  silicate network remains intact. In contrast, the increase in intensity

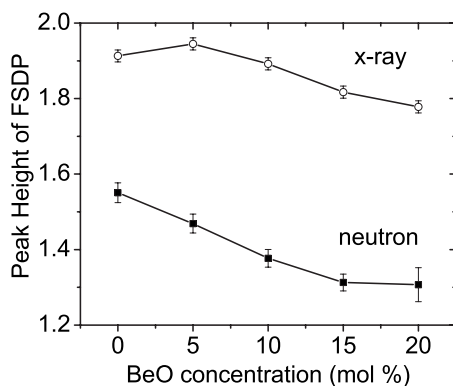


FIG. 10. Variation in the FSDP height of the x-ray and neutron structure factors for  $x\text{BeO}+(1-x)\text{SiO}_2$  glasses. The dashed line represents the height of the neutron FSDP scaled by  $\text{SiO}_2$  content.

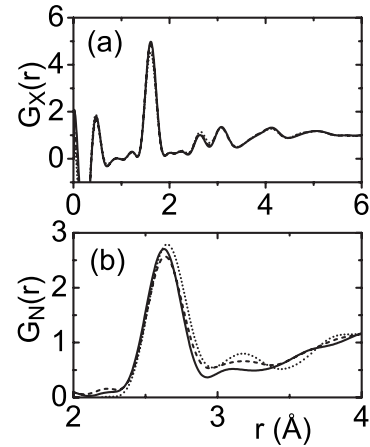


FIG. 11. Total (a) x-ray- and (b) neutron-diffraction radial distribution functions for pure  $\text{SiO}_2$  glass (solid line), 10%BeO-90% $\text{SiO}_2$  glass (dashed line), and glass 20%BeO-80% $\text{SiO}_2$  (dotted line).

at 3.18  $\text{\AA}$  with increasing BeO concentration in the neutron radial distribution function is attributed to Be-O correlations since in the BeO crystal structure, the Be-O2 correlation distance for three-membered rings is at 3.15  $\text{\AA}$ . This will be the subject of a future paper.

## V. SUMMARY

The techniques of isotopic substitution in neutron diffraction and high-energy x-ray diffraction have been applied to determine the partial structure factors of vitreous  $\text{SiO}_2$ . The experimental partial structure factors and corresponding pair distribution functions are in reasonable agreement with previously published *ab initio*<sup>21</sup> and classical molecular-dynamics<sup>26</sup> simulations, although the extracted average  $\angle\text{Si-O-Si}$  angle of  $148.5 \pm 2.0^\circ$  is somewhat higher than predicted by the simulations. The average  $\angle\text{Si-O-Si}$  angle is however in good agreement with the results of NMR studies which yield  $147^\circ$  and  $151^\circ$ .<sup>27,28</sup>

The Faber-Ziman and Bhatia-Thornton partial structure factors have been used to test two different models of intermediate range order (and hence the origin of the FSDP) in vitreous  $\text{SiO}_2$ . A void-cluster model predicting a first sharp diffraction peak in the concentration-concentration partial structure factor<sup>12</sup> is not observed in the experimental functions.<sup>12</sup> However, the Faber-Ziman partial structure factors are consistent with a FSDP which arises from the periodicity of boundaries between a succession of small cages in the network. This cage model is used to explain the compositional dependence of the FSDP height in neutron- and x-ray-diffraction data on BeO- $\text{SiO}_2$  glasses, in which  $\text{BeO}_4$  tetrahedra enter into the voids within the  $\text{SiO}_2$  network.

Finally, this work has shown that with accurate, stable neutron instrumentation it is possible to extend the method of isotopic substitution to include Si, and we have extracted a more accurate value for the coherent neutron-scattering length of  $^{29}\text{Si}$ , namely,  $b(^{29}\text{Si})=4.80(5)$  fm. We anticipate that this will become a useful parameter in future low-contrast  $^{29}\text{Si}$  neutron-scattering experiments, made possible

by high-flux instruments at the intense neutron sources currently being built worldwide.

#### ACKNOWLEDGMENTS

This work at Argonne National Laboratory was supported

by the U.S. DOE, under Contract No. DE-AC02-06CH11357. S.S. would like to acknowledge funding from NSF Grant No. DMR-0603933. J.L.Y. acknowledges the NSF (Grant No. CHE 0094202), the DOE (Grant No. DE-FG2-05ER46235), and the Carnegie/DOE Alliance Center for support.

- 
- <sup>1</sup>A. C. Wright, *J. Non-Cryst. Solids* **179**, 84 (1994).  
<sup>2</sup>S. R. Elliott, *Nature (London)* **354**, 445 (1991).  
<sup>3</sup>P. S. Salmon, R. A. Martin, P. E. Mason, and G. J. Cuello, *Nature (London)* **435**, 75 (2005).  
<sup>4</sup>W. H. Zachariasen, *J. Am. Chem. Soc.* **54**, 3841 (1932).  
<sup>5</sup>A. C. Wright, *Phys. Chem. Glasses* **49**, 103 (2008).  
<sup>6</sup>B. E. Warren, H. Krutter, and O. Morningstar, *J. Am. Ceram. Soc.* **19**, 202 (1936).  
<sup>7</sup>D. L. Price, M.-L. Saboungi, and A. C. Barnes, *Phys. Rev. Lett.* **81**, 3207 (1998).  
<sup>8</sup>S. C. Moss and D. L. Price, in *Physics of Disordered Materials*, edited by D. Adler, H. Fritzsche, and S. Ovshinky (Plenum, New York, 1985), p. 77.  
<sup>9</sup>D. L. Price, S. C. Moss, R. Reijers, M. L. Saboungi, and S. Susman, *J. Phys.: Condens. Matter* **1**, 1005 (1989).  
<sup>10</sup>P. S. Salmon, A. C. Barnes, R. A. Martin, and G. J. Cuello, *Phys. Rev. Lett.* **96**, 235502 (2006).  
<sup>11</sup>J. Urquidi, C. J. Benmore, J. Neufeind, and B. Tomberli, *J. Appl. Crystallogr.* **36**, 368 (2003).  
<sup>12</sup>S. R. Elliott, *J. Phys.: Condens. Matter* **4**, 7661 (1992).  
<sup>13</sup>S. Kohara and K. Suzuya, *J. Phys.: Condens. Matter* **17**, S77 (2005).  
<sup>14</sup>J. Tao, C. J. Benmore, T. G. Worlton, J. M. Carpenter, D. Mikkelson, R. Mikkelson, J. Siewenie, J. Hammonds, and A. Chatterjee, *Nucl. Instrum. Methods Phys. Res. A* **562**, 422 (2006).  
<sup>15</sup>V. F. Sears, *Neutron News* **3**, 26 (1992).  
<sup>16</sup>L. Koester, K. Knopf, and W. Waschkowski, *Z. Phys. A* **289**, 399 (1979).  
<sup>17</sup>T. E. Faber and J. M. Ziman, *Philos. Mag.* **11**, 153 (1965).  
<sup>18</sup>J. E. Enderby, D. M. North, and P. A. Egelstaff, *Philos. Mag.* **14**, 961 (1966).  
<sup>19</sup>See EPAPS Document No. E-PRBMD0-78-023838 for the tabulated values for the curves in Fig. 1. For more information on EPAPS, see <http://www.aip.org/pubservs/epaps.html>.  
<sup>20</sup>P. Vashishta, R. K. Kalia, J. P. Rino, and I. Ebbsjo, *Phys. Rev. B* **41**, 12197 (1990).  
<sup>21</sup>J. Sarnthein, A. Pasquarello, and R. Car, *Phys. Rev. Lett.* **74**, 4682 (1995).  
<sup>22</sup>J. Sarnthein, A. Pasquarello, and R. Car, *Phys. Rev. B* **52**, 12690 (1995).  
<sup>23</sup>P. Johnson, A. C. Wright, and R. N. Sinclair, *J. Non-Cryst. Solids* **58**, 109 (1983).  
<sup>24</sup>R. L. Mozzi and B. E. Warren, *J. Appl. Crystallogr.* **2**, 164 (1969).  
<sup>25</sup>J. Neufeind and K.-D. Liss, *Ber. Bunsenges. Phys. Chem.* **100**, 1341 (1996).  
<sup>26</sup>J. P. Rino, I. Ebbsjo, R. K. Kalia, A. Nakano, and P. Vashishta, *Phys. Rev. B* **47**, 3053 (1993).  
<sup>27</sup>F. Mauri, A. Pasquarello, B. G. Pfrommer, Y. G. Yoon, and S. G. Louie, *Phys. Rev. B* **62**, R4786 (2000).  
<sup>28</sup>T. M. Clark, P. J. Grandinetti, P. Florian, and J. F. Stebbins, *Phys. Rev. B* **70**, 064202 (2004).  
<sup>29</sup>S. Sampath, C. J. Benmore, K. M. Lantzky, J. Neufeind, K. Leinenweber, D. L. Price, and J. L. Yarger, *Phys. Rev. Lett.* **90**, 115502 (2003).  
<sup>30</sup>A. B. Bhatia and D. E. Thornton, *Phys. Rev. B* **2**, 3004 (1970).  
<sup>31</sup>J. Bletry, *Philos. Mag. B* **62**, 469 (1990).  
<sup>32</sup>C. Massobrio and A. Pasquarello, *J. Chem. Phys.* **114**, 7976 (2001).  
<sup>33</sup>P. S. Salmon, *J. Non-Cryst. Solids* **353**, 2959 (2007).  
<sup>34</sup>J. H. Lee and S. R. Elliott, *Phys. Rev. B* **50**, 5981 (1994).  
<sup>35</sup>S. Sen and P. Yu, *Phys. Rev. B* **72**, 132203 (2005).  
<sup>36</sup>D. L. Price, A. J. G. Ellison, M. L. Saboungi, R. Z. Hu, T. Egami, and W. S. Howells, *Phys. Rev. B* **55**, 11249 (1997).